Scaling behavior in very small percolation lattices

J. B. Elliott, M. L. Gilkes, J. A. Hauger, A. S. Hirsch, E. Hjort, N. T. Porile, R. P. Scharenberg, B. K. Srivastava, M. L. Tincknell, and P. G. Warren
Departments of Physics and Chemistry, Purdue University, West Lafayette, Indiana 47907
(Received 19 June 1996)

We examine the average cluster distribution as a function of lattice probability for a very small ($L=6$) lattice and determine the scaling function of three-dimensional percolation. The behavior of the second moment, calculated from the average cluster distribution of $L=6$ and $L=63$ lattices, is compared to power-law behavior predicted by the scaling function. We also examine the finite-size scaling of the critical point and the size of the largest cluster at the critical point. This analysis leads to estimates of the critical exponent ν and the ratio of critical exponents β/ν. [S0556-2813(97)02703-9]

PACS number(s): 25.70.Pq, 64.60.Ak, 24.60.Ky, 05.70.Jk

I. INTRODUCTION

Much interest in critical phenomena in small systems has been generated by recent work in nuclear physics [1–13]. The idea that nuclear multifragmentation, the breakup of nuclei due to high-energy collisions into several intermediate mass fragments, can be viewed as a critical phenomenon as observed in fluid, magnetic, and other systems prompts several questions. Of particular importance is the question as to whether or not the signals of phase transitions existing in systems in the thermodynamic limit persist to systems with a few hundred constituents. If the signals do persist, then what methods can be employed to find them? What observables can be used as control parameters?

In an attempt to answer these questions this work examines the behavior of cluster distributions of small percolation lattices. Using data from a small lattice the scaling function of three-dimensional percolation is determined. Using the scaling function, various power laws are predicted that describe the behavior of the lattice near the critical point. These predictions are compared to the observed behavior of percolation data from small and large lattices. The method of γ-matching to determine critical exponents introduced in a previous paper on percolation [14] and used to determine exponent values of nuclear multifragmentation in [11] is used on a small percolation lattice. Next, the number of clusters, i.e., the multiplicity M, is used as the control parameter and a scaling function based on this version of the control parameter is found. Using the scaling function power laws are predicted and compared to the measured behavior of percolation data. Finally, finite-size scaling effects are investigated as the size of the lattice is decreased.

II. DESCRIPTION OF PERCOLATION

This work continues the efforts of previous examinations of small percolation lattices in [14] and investigates the scaling behavior of bond building percolation on very small simple cubic lattices in three dimensions with open boundary conditions. In this study cluster distributions of percolation lattices were generated in a standard fashion by forming bonds between sites. Bonds were either active (on) or inactive (off) according to the following algorithm.

The control parameter for percolation is the lattice probability, p_l. A single value of p_l was randomly chosen for the entire lattice. All probabilities were between 0 and 1. Next, a bond probability p_{bi} was randomly chosen for each bond. If p_{bi} was less than p_l then the ith bond was active (on) and two sites were joined in a cluster.

At a low value of p_l few bonds were formed resulting in many small clusters, yielding a distribution that is analogous to the gaseous phase of a fluid. At a high value of p_l many bonds were formed and there were a few large clusters. This is analogous to the liquid phase of a fluid. In an infinite lattice the phase transition occurs at a unique value of the lattice probability p_c and is defined as the value of p_l when the probability of forming a spanning or percolating cluster changes from zero to unity.

The behavior of the average cluster distribution, the number of clusters of size s per lattice site, was examined as a function of p_l for a lattice of side $L=6$; the total number of sites is then $s_0 = 216$. The average cluster distribution was generated by computing 100 000 realizations of the lattice letting p_l vary uniformly between 0 and 1. The resulting cluster distributions were histogrammed into 100 bins in p_l yielding cluster distributions $n_s(p_l)$ that were *averaged* over a range of 0.01, the width of one bin, in p_l. This averaging scheme serves to smear the cluster distribution in a manner that may be analogous to how the fragment distributions of nuclear multifragmentation are smeared. In nuclear multifragmentation the event's charged particle multiplicity is used as the control parameter instead of the temperature of the system [11,12,17], which is the usual control parameter for thermodynamic systems. While the multiplicity is linearly related to the temperature of the system [13], there is a spread in temperatures at a given multiplicity. By averaging over some range in p_l it is possible to include a smearing effect in the analysis of percolation data that is, to the lowest order, reminiscent of the smearing present in nuclear multifragmentation.

III. DETERMINING THE SCALING FUNCTION OF THREE-DIMENSIONAL PERCOLATION USING A SMALL ($L=6$) LATTICE

In general the cluster distribution of any percolation lattice is written as [15]

TABLE I. Summary of results for percolation studies.

Quantity	$L=\infty$	$L=63$ [14]	$L=6$ [14]	$L=6$ (γ match)	$L=6$ (p_l)	$L=6$ (M)	FS Scaling
$p_c(L)$	0.2488	0.254185 ± 0.00005	0.33813 ± 0.00007	0.33 ± 0.02	0.310 ± 0.005	54	
β	0.41	0.46 ± 0.02					0.41 ± 0.02
γ	1.80	1.87 ± 0.02	1.728 ± 0.007	1.7 ± 0.2			
σ	0.45		0.50 ± 0.04				
ν	0.88						0.93 ± 0.03
τ	2.18	2.20 ± 0.05	2.16 ± 0.02		2.208 ± 0.003		
β/ν	0.47						0.44 ± 0.01
C_+/C_-	8.0			11 ± 10	7.85	19.7	
$f(z_c)$	1.0				1.02	0.98	
$f(z_{\max})$	1.6				1.77	1.82	
$z_{\max}$	-0.8				-0.76	-2.24	
ϵ_+ (far)			-0.4032	-0.41 ± 0.06			
ϵ_+ (near)			-0.2020	-0.21 ± 0.05			
ϵ_- (far)			-0.2020	0.17 ± 0.04			
ϵ_- (near)			0.3736	0.42 ± 0.09			

$$n_s(p_l)=q_0 s^{-\tau} f(z), \tag{1}$$

where $n_s(p_l)$ is the number of clusters of size s per lattice site at a lattice probability p_l, $f(z)$ is the scaling function, $z=s^{\sigma}\epsilon$ is the scaling variable, $\epsilon=[p_l-p_c(L)]/p_c(L)$, $p_c(L)$ is the critical probability for a lattice of side L, and q_0 is a normalization constant that depends only on the value of τ [16].

The specific form of the scaling function is unknown analytically. However, empirical examinations of large ($s_0>10^6$) lattices have shown some general features [15,16]. At the critical point ($z=z_c=0$) the cluster distribution is described by a simple power law so that $f(z)=1$. The scaling function has a single maximum at $z=z_{\max}$; for three-dimensional percolation, $f(z_{\max})=1.6$ and $z_{\max}\sim-0.8$ [15].

The single maximum in $f(z)$ has two important consequences. The first yields a method for determining the critical exponent σ. At the maximum of the scaling function the scaling variable is constant, which leads to a power law relating the position, as a function of ϵ, the maximum in production of s-sized clusters and the cluster size. This power law was used to determine σ for three-dimensional percolation in [14] and for the multifragmentation of gold nuclei in [12]. Results for percolation are summarized in Table I.

The second consequence of a single maximum of the scaling function is that attempts to determine the critical point by fitting the cluster distribution to a simple power law and finding a minimum in the effective exponent will generally fail. Writing the cluster distribution in terms of an effective exponent yields

$$n_s(p_l)=q_0 s^{-\tau} f(z)=A s^{-\tau_{\rm eff}}, \tag{2}$$

where A is a free-floating normalization factor. Solving Eq. (2) for $\tau_{\rm eff}$ and taking the derivative with respect to z shows that the minimum in $\tau_{\rm eff}$ occurs at the maximum in $f(z)$, which is not, in general, at the critical probability. This misconception has been perpetuated in the multifragmentation literature [18–22].

To determine the form of the scaling function ratio [15,16] $n_s(p_l)/q_0 s^{-\tau}$ was isolated and plotted versus z for all values of p_l and for clusters where $1\%<s/s_0<12\%$. The resulting plot clearly shows the collapse of the data onto a single curve as required by Eq. (1), see Fig. 1. The infinite lattice three-dimensional percolation values of the critical exponents τ and σ are used in $n_s(p_l)/q_0 s^{-\tau}$ and z; these values are in good agreement with those determined in previous efforts with small percolation lattices [14].

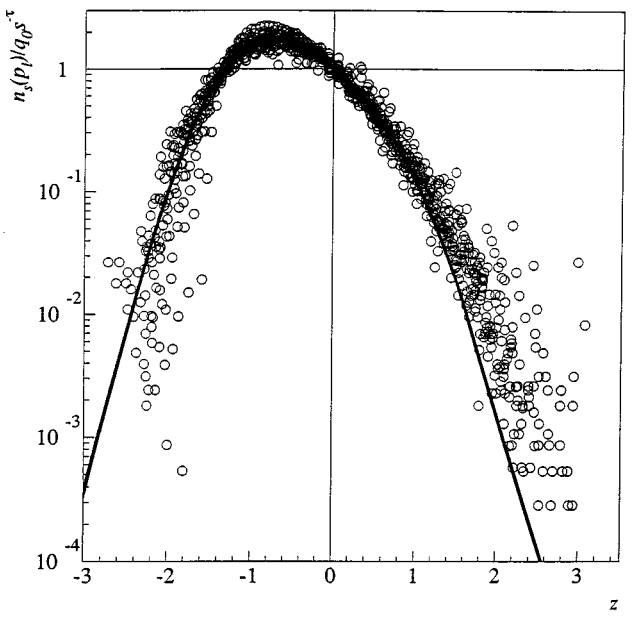

FIG. 1. Data from an $L=6$ three-dimensional simple cubic lattice are plotted to give the form of the scaling function intrinsic to percolation in three dimensions. The solid line is a fit to the data. $p_c(6)=0.31$.

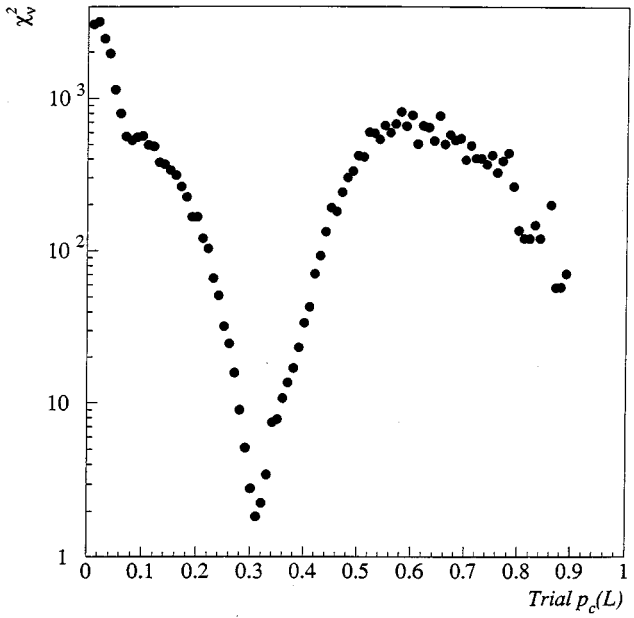

FIG. 2. The χ^2_ν that results from fitting the cluster distribution at a particular value of the p_l. χ^2_ν drops more than three orders of magnitude to a minimum at the critical probability. This analysis indicates $p_c(6)=0.31$.

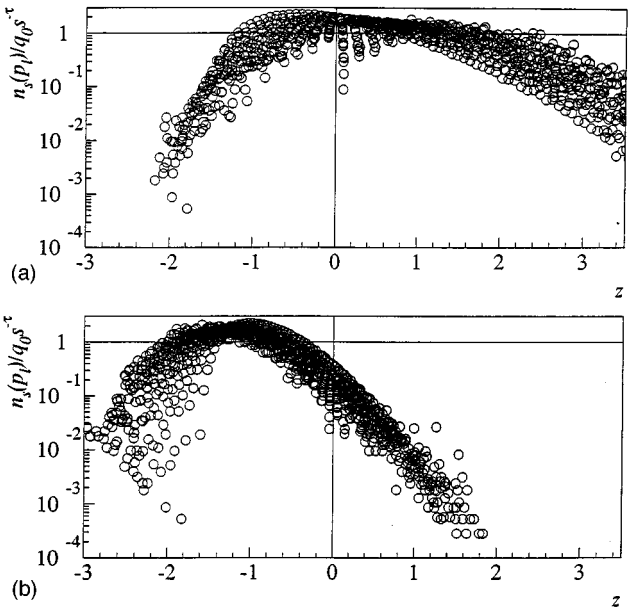

FIG. 3. (a) Data from an $L=6$ three-dimensional simple cubic lattice plotted in the same manner as in Fig. 1, but with $p_c(6)-0.1=0.21$. (b) The same plot with $p_c(6)+0.1=0.41$. Note that in neither plot do the data exhibit the collapsing behavior as in Fig. 1, nor do the data go through the point (0,1).

For the scaling variable z the value of $p_c(L)$ was determined by fitting the average cluster distribution at each value of p_l to the simple power law that describes the cluster distribution at the critical point. The only free-floating parameter in these fits was the exponent τ. Again, q_0 is an overall normalization depending solely on the value of τ [16]. The resulting χ^2_ν of the fits were examined. Figure 2 shows a drop in χ^2_ν of over three orders of magnitude. This is a clear indication of the location of the critical point and the value of $p_c(L)$. This value of $p_c(L)$ and the τ value of the resulting fit are within 10% of the values determined in [14]; see Table I.

While the plot of $n_s(p_l)/q_0 s^{-\tau}$ versus z is relatively insensitive to the choice of τ and σ, it is very sensitive to the choice of $p_c(L)$. If the value of $p_c(L)$ is changed by 0.1 the data no longer collapse onto a single curve, nor do they pass through the critical point $f(z_c)=1$; see Figs. 3(a) and 3(b).

It has been suggested that $f(z)\sim\exp[-c(z-z_{\max})^2]$, where c is some constant [15]. However, the $L=6$ data are asymmetric about the maximum so that the averaged cluster distribution data were fit to the sum of two Gaussians. The best fit was found to be

$$f(z)=C_1 e^{-(1/2)(z-\mu_1/\sigma_1)^2}+C_2 e^{-(1/2)(z-\sigma_2/\mu_2)^2} \qquad (3)$$

by minimizing χ^2_ν. See Table II for parameter values. For this functional form $f(z_c)=1.02$, $f(z_{\max})=1.77$, and $z_{\max}=-0.76$. Table I shows the comparison between published values for large lattices and those determined in this work. The agreement between the quantities determined here and the accepted values, within 10%, is evidence that the form of the scaling function determined here, using a small lattice $L=6$, is the scaling function for all of three-dimensional percolation. Thus it is possible to observe infinite lattice critical behavior in a small system in spite of its size and any effects due to the smearing introduced by histogramming the data in p_l.

IV. DETERMINING POWER LAWS FROM THE SCALING FUNCTION

With the form of the scaling function determined, it is possible to derive all other critical behavior for three-dimensional percolation. This includes the determination of power laws, critical exponents and, in particular, the constants of normalization.

The simplest example of this is the power law at the critical point, which is a consistency check since $p_c(L)$ was chosen such that the cluster distribution was well described by a power law, though whether or not the infinite lattice value of τ actually describes the behavior of the data is an open question. When the scaling function goes to unity at the critical point we are left with

$$n_s[p_c(L)]=q_0 s^{-\tau}. \qquad (4)$$

Figure 4(a) shows the agreement between this power law, using the infinite lattice values for τ and q_0, and the $L=6$ averaged cluster distribution data at the critical point. This

TABLE II. Scaling function parameters.

C_1	0.94412
μ_1	−0.94303
σ_1	0.43714
C_2	1.0838
μ_2	−0.36831
σ_2	0.65575

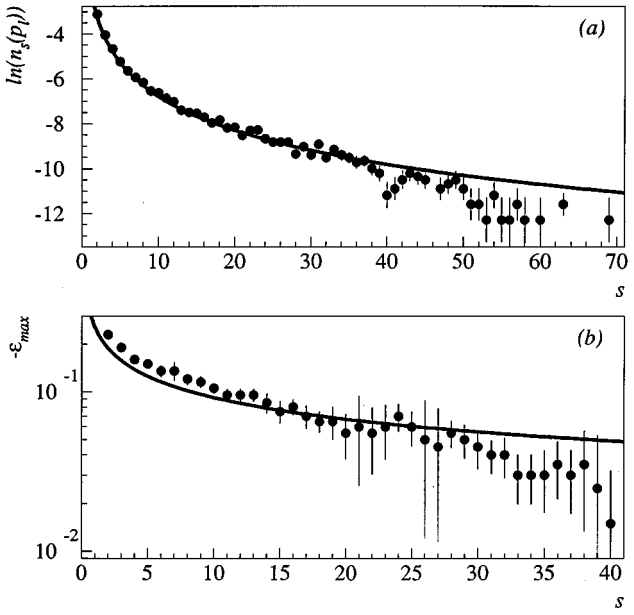

FIG. 4. (a) The cluster distribution at $p_c(6)=0.31$ for an $L=6$ three-dimensional simple cubic percolation lattice. Solid circles are data points and the solid line is the power law predicted in Eq. (1) using the canonical three-dimensional percolation value of τ. The line is *not* a fit to the data. (b) Data from the $L=6$ lattice for the σ power law plotted as solid circles. The solid line is the power law predicted from Eq. (6), not a fit to the data. Canonical values of $\epsilon_{\max}$ and σ are used.

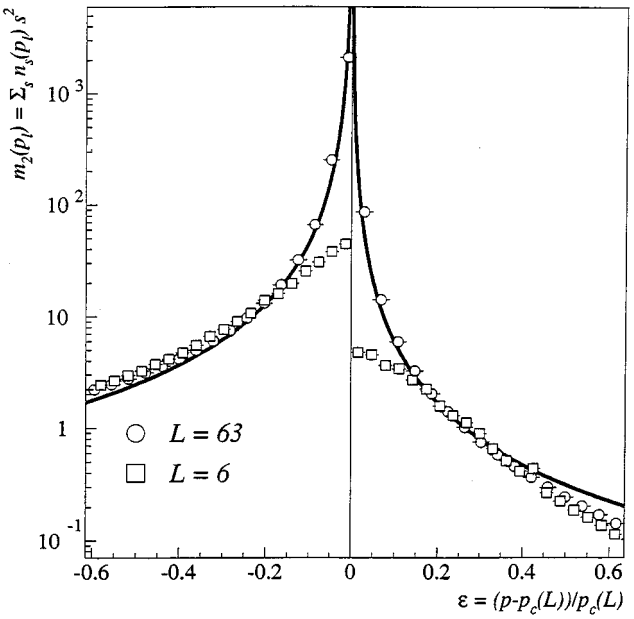

FIG. 5. Measured second moment data from an $L=63$ simple cubic lattice (open circles) and from an $L=6$ lattice (open squares) as a function of ϵ. $p_c(63)=0.254185$, $p_c(6)=0.31$. The solid lines are the γ-power laws predicted by using the form of the scaling function as determined in Fig. 1 from the $L=6$ data and Eq. (8). Note the agreement between the larger lattice and the power law predicted from the smaller lattice data.

result gives credence to the use of the infinite lattice value of τ when determining the scaling function.

The σ-power law is nearly as simple. At $z_{\max}$ we have

$$z_{\max}=s^{\sigma}\epsilon_{\max}=s^{\sigma}[p_{\max}(s)-p_c(L)]/p_c(L), \tag{5}$$

where $p_{\max}(s)$ is the value of the lattice probability at which there is a maximum in the production of s-sized clusters. Dividing through by s^{σ} give the following power law:

$$-\epsilon_{\max}=z_{\max}s^{-\sigma}. \tag{6}$$

Figure 4(b) shows the agreement between this power law and the $L=6$ average cluster distribution data at $z_{\max}$. Again the data is well described by a power law with exponent values equal to their infinite lattice values, which is in keeping with the method of determination of the scaling function.

A dramatic example of the predictive power of the scaling function is the derivation of the power law that describes the divergence of the second moment, $m_2(p_l)=c_{\pm}|\epsilon|^{-\gamma}$. The second moment is defined as

$$m_2(p_l)=\sum_{s=1}^{s_\infty} n_s(p_l)s^2, \tag{7}$$

where the sum runs over all clusters except the spanning cluster s_∞. By substituting Eq. (1) into Eq. (7), letting the sum be replaced by an integral, and changing the variable of integration from s to z we find

$$M_2(\epsilon)=\left|\frac{q_0}{\sigma}\int_{-\infty}^{\infty}|z|^{3-\tau-\sigma/\sigma}f(z)dz\right||\epsilon|^{\tau-3/\sigma}. \tag{8}$$

The constants of normalization, C_+ for the gaseous region and C_- for the liquid region, are determined by evaluating the term in the brackets and the exponent γ is thus defined as a ratio that depends on the values of τ and σ. The ratio of C_+ to C_- computed here is 7.85 as compared to 8.0 in [15].

Figure 5 shows the agreement with the predicted power law and the measured second moment percolation data from lattices of side $L=6$, 63; $s_0=216$, 250 047. The agreement between the predicted power law and the $L=63$ lattice is particularly noteworthy. Thus, using a small lattice the behavior of a large lattice is predicted. Infinite lattice critical behavior has been observed in small systems.

It is also of import to note in Fig. 5 that for the $L=6$ lattice there exists some range in ϵ where the behavior of the second moment is well described by the γ power law. As is expected, too far from the critical point neither lattice is well described by the power law. Too near the critical point and manifestations of finite size effects in the data for the small lattices can be observed. Below, methods are developed to determine this effective power law range in ϵ based on the γ matching introduced in [11].

V. γ-MATCHING RESULTS FOR THE AVERAGE CLUSTER DISTRIBUTION

In previous work the method for determining critical exponent values and the location of the critical point from the cluster distribution was based on a method of matching exponent values on both sides of the critical point [11,14]. The idea was to find the regions where the power-law behavior predicted by the scaling function holds. As is seen in Fig. 5 there is some intermediate ϵ region where the second mo-

ment data is described by a power law. However, at ϵ values too close to the critical point the power-law behavior is modified by finite-size effects, while at ϵ values too far from the critical point the scaling assumptions implicit in power-law behavior are no longer valid. In earlier percolation studies [14] general guidelines based on the correlation length and size of the fluctuations were used. In a previous nuclear multifragmentation analysis [11] it was impossible to use such guidelines. To that end a method was developed that could search for regions best fit by power laws as well as to determine the location of the critical point. The values of the critical exponents and the normalizations involved in the power laws were obtained from the best fit power laws in those regions.

The method is as follows. Trial boundaries for power-law regions were chosen along with a value of the critical point. This leads to five parameters that are chosen for each set of power-law regions examined. In the work on percolation lattices detailed in this paper these are $\epsilon(\text{far})_{\pm}$, $\epsilon(\text{near})_{\pm}$, and $p_c(L)$. (Far) denotes the further point in either region from the critical point and (near) indicates the closest approach to the critical point; ''+'' denotes the boundaries for the power-law fit region on the gas side of the critical point and ''−'' refers to the power-law fit region on the liquid side of the critical point. In this work approximately 45 000 different regions were examined. For each region a power law was fit to the second moment data and a value of γ_+, C_+, $\chi^2_{\nu+}$, γ_-, C_-, and $\chi^2_{\nu-}$ were determined.

Power-law fit regions and critical point locations were evaluated by demanding that (i) they yield γ_+ and γ_- values that match each other to within the error bars on those values returned by the fitting routine and (ii) that the χ^2_ν of the fits are in the bottom half of the distribution. The results from the power-law fit regions that passed these two criteria were then histogrammed and average values for all quantities concerned were determined. The results are summarized in Table I.

The value of γ determined in this manner is within 10% of the value determined in [14] and the infinite lattice value. The ratio of C_+/C_- determined with this method is also in agreement with the infinite lattice value and the values predicted by the scaling function. The value of $p_c(L)$ determined here is also within a few percent of the value determined in a previous analysis of the $L=6$ lattice [14] and the value determined above by looking for a pure power law in the cluster distribution.

Figure 6 shows the fit regions determined with the γ-matching method. The fit regions determined in this manner are in good agreement with what is determined by a visual inspection of Fig. 5. The boundaries of the fit regions are also the same, to within error bars, as those used in the previous percolation effort [14]; see Table I.

VI. USING CLUSTER MULTIPLICITY AS THE CONTROL PARAMETER

In the previous section the lattice probability was used as the control parameter. In a thermodynamic system the temperature of the system is generally used as the control parameter. In nuclear multifragmentation temperature is also

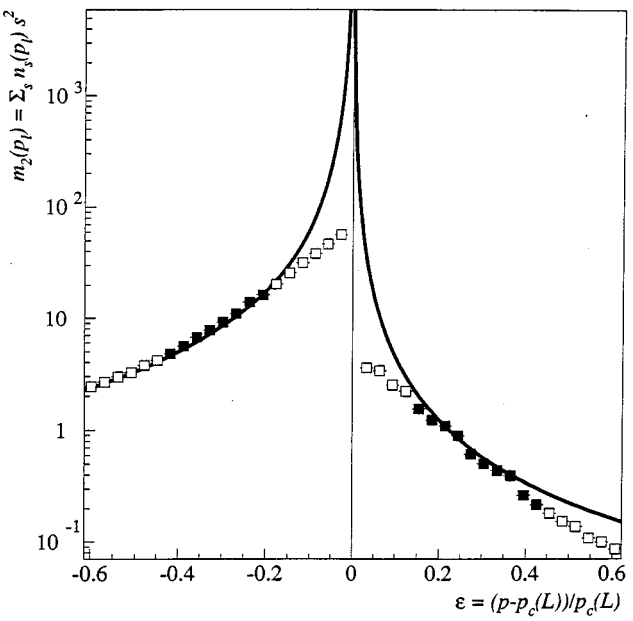

FIG. 6. Results of the γ-matching method for the measured second moment data for the $L=6$ lattice. $p_c(6)=0.33$. Solid squares show the average fit regions on both sides of the critical point. The solid lines are the power laws determined from the fits.

the intrinsic control parameter, however, it is not a direct observable. It was suggested that an event's charged particle multiplicity is a reasonable choice of observables to use as the control parameter [17]. This choice is supported by the linear relation between the temperature and event charged particle multiplicity observed in nuclear multifragmentation [13] and the consistent results obtained in the extraction of critical exponent values in the multifragmentation of gold nuclei [11,12].

For percolation lattices it is possible to study the results of choosing different control parameters directly. For three-dimensional bond building percolation on a simple cubic lattice there is not a linear relation between the cluster multiplicity M and the lattice probability p_l, see Fig. 7. The analysis of the previous section was repeated with M as the control parameter, such that $\epsilon=[M_c(L)-M]/M_c(L)$, where $M_c(L)$, the *critical multiplicity*, is the number of clusters at the critical point and is estimated from the average cluster multiplicity at $p_c(L)$.

The average cluster distribution was generated by histogramming the 100 000 realizations of the lattice in bins according to cluster multiplicity. The averaged cluster distribution is now written as

$$n_s(M)=q_0 s^{-\tau} f(z). \tag{9}$$

The scaling function was determined as before by plotting the ratio $n_s(M)/q_0 s^{-\tau}$ against the scaling variable z, which now depends on $\epsilon(M)$. Figure 8 shows that the data for the $L=6$ lattice still collapses onto a single curve as Eq. (9) requires. Examining the properties of the resulting form of the scaling function shows, $f(z_c)=0.98$, $f(z_{\max})=1.82$, and $z_{\max}=-2.24$. The first two agree well with published values, see Table I, while the last shows more disagreement. This is not unexpected since the abscissa has changed from

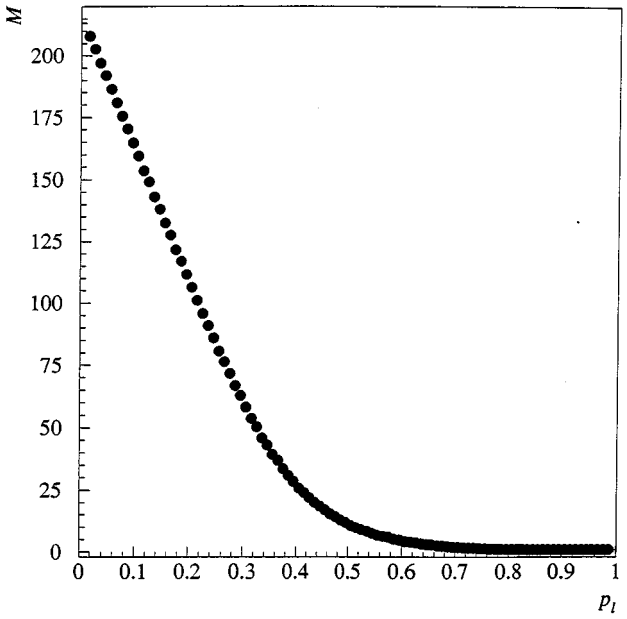

FIG. 7. Cluster multiplicity M as a function of lattice probability p_l.

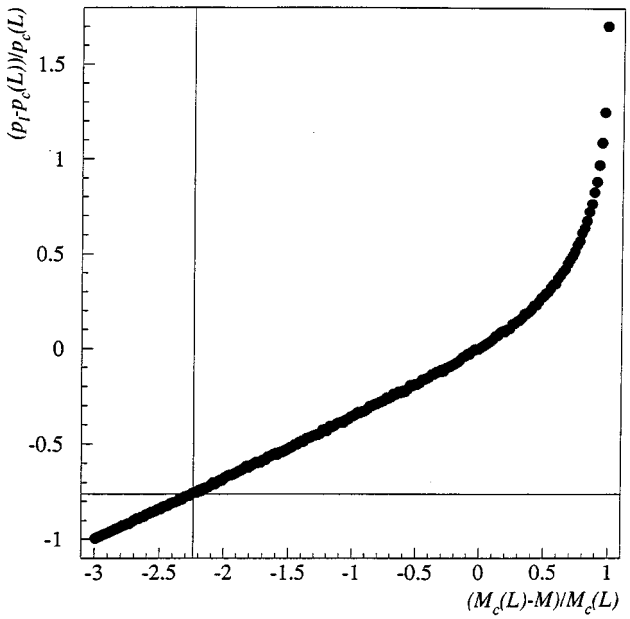

FIG. 9. $\epsilon(p_l)$ as a function of $\epsilon(M)$. The maximum of the scaling function $\epsilon_{\max}(p_l)$ is shown as the horizontal line. The maximum of the scaling function $\epsilon_{\max}(M)$ is shown as the vertical line. The maximum of the scaling function is the same point in either mapping of ϵ.

Fig. 1 to Fig. 8. Even though the quantity ϵ is a ratio, due to the subtraction in the numerator, constants of proportionality and other factors relating p_l and M do not cancel. Figure 9 shows the relation between $\epsilon(p_l)$ and $\epsilon(M)$ for an $L=6$ lattice. Lines are drawn to indicate the location of $z_{\max}(p_l)$ and $z_{\max}(M)$. It is clear that the maximum in the scaling function has the same location in either mapping of ϵ. The data from the $L=6$ percolation lattice exhibit scaling behavior regardless of the choice of ϵ, which indicates that it makes little difference whether lattice probability or cluster multiplicity is used as the control parameter.

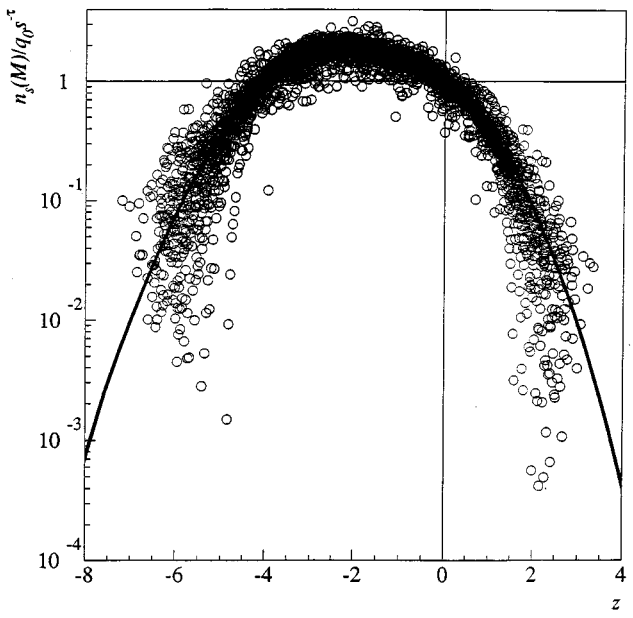

FIG. 8. Data from an $L=6$ three-dimensional simple cubic lattice plotted to give the form of the scaling function intrinsic to percolation in three dimensions using the cluster multiplicity as the control parameter. The solid line is a fit to the data.

When the power law describing the divergence of $m_2(M)$ is determined from Eq. (9) the same agreement between the measured system size and the predicted power law is observed. Figure 10 shows the comparison of data from lattices of side $L=6$, 63 and the power law predicted from the fit to the data for an $L=6$ lattice shown in Fig. 8. While the power law predicted by the scaling function of Eq. (9) yields, by definition, the same value for γ as previously, the ratio of C_+/C_- is 19.7, different from the results of the previous analysis and the accepted value. The difference in this ratio is due to the difference in the abscissa when changing from $\epsilon(p_l)$ to $\epsilon(M)$. The observed behavior of the second moment for the lattices in Fig. 10 supports these results. This indicates that the values of the constants of normalization depend on the choice of control parameter, but the values of exponents do not. This is seen explicitly in the derivation of Eq. (8) from either Eq. (1) or Eq. (9). The critical exponent γ is, by definition, a function of the exponents σ and τ and does not depend on the choice of $\epsilon(p_l)$ or $e(M)$.

It is also possible to map the fit regions, $\epsilon(\text{far})_{\pm}$ and $\epsilon(\text{near})_{\pm}$, determined from the γ-matching procedure, from p_l to M using Fig. 9. The fit regions, dependent on M, are in good agreement with fit regions determined from a visual inspection of Fig. 10. Again, this indicates that the use of multiplicity as a control parameter does not interfere with the determination of the values of critical exponents.

VII. FINITE-SIZE SCALING RESULTS

In previous percolation work [14], data from the critical point was avoided because it was most severely affected by

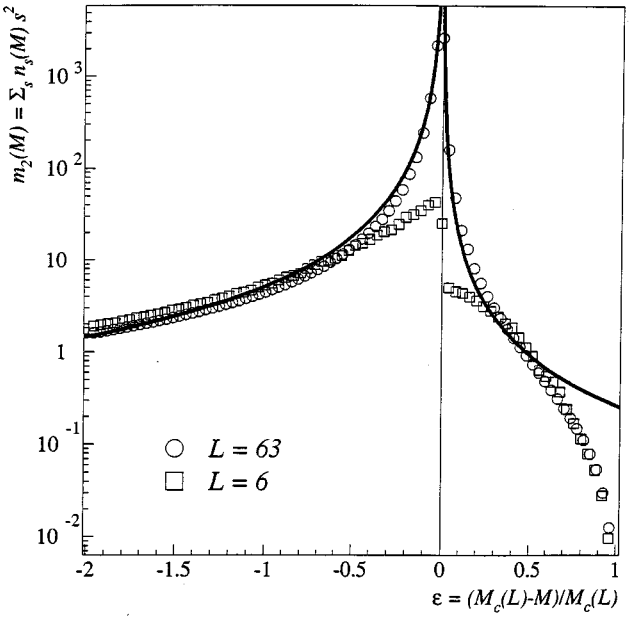

FIG. 10. Measured second moment data plotted as open circles for an $L=63$ simple cubic lattice and as open squares for an $L=6$ lattice as a function of ϵ. $M_c(63)=67\,610$, $M_c(6)=54$. The solid lines are the γ-power laws predicted from using the form of the scaling function as determined in Fig. 9 for the $L=6$ data and Eq. (8). Note the agreement between the larger lattice and the power law predicted from the smaller lattice data.

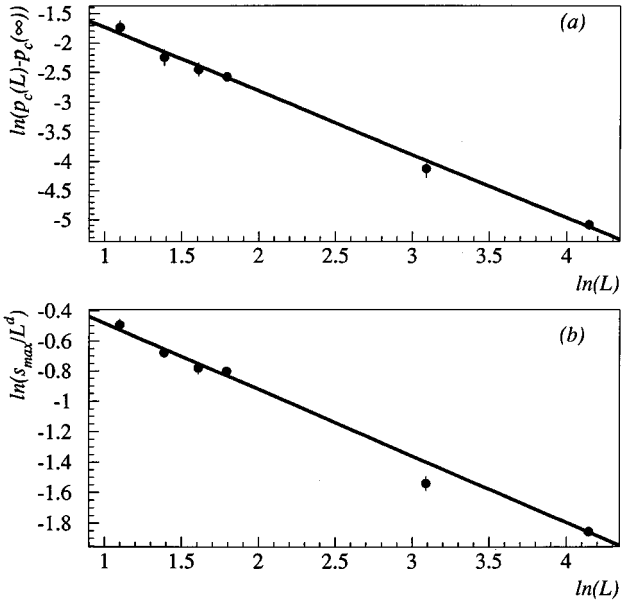

FIG. 11. (a) Finite size scaling effects on the critical point: the location of the critical point depends of the lattice size via a power law with the exponent ν. (b) Finite-size scaling of the size of the largest cluster: the size of the largest cluster at the critical point depends on the lattice size via a power law with the exponent β/ν.

the finite size of the systems in question. Now, methods are employed to determine the value of the critical exponent ν and the ratio β/ν based on the effects of the finite size of the system.

In percolation lattices the location of the critical point changes as a function of system size [23,24]. The percolation phase transition occurs when the probability R of finding a spanning cluster reaches unity. In a lattice of infinite extent this is a step function. In finite-size lattices the step function is smoothed out over a range in lattice probability. As the lattice size decreases the critical point is spread out and becomes a critical region and the value of the lattice probability at which R reaches one $p_c(L)$ increases. Thus the value of $p_c(L)$ increases as the lattice size decreases. This phenomenon is known as the finite-size scaling of the critical point and is described by [23]

$$p_c(L)-p_c(\infty)\sim L^{-1/\nu}. \tag{10}$$

Thus the value of the critical exponent ν can be determined from the finite-size scaling of the critical point via Eq. (10) if the value of $p_c(L)$ is known for lattices of varying sizes.

For the lattices with 216 and 250 047 sites the values of $p_c(L)$ determined by γ-matching results [14] were used. Estimates of $p_c(L)$ for the other lattices (27, 64, 125, and 10 648; $L=3$, 4, 5, and 22) were made based on the location of the maximum in the fluctuations of the largest cluster. Cluster distributions from lattice realizations were binned in p_l so that an error of $\pm$ half a bin width is associated with this estimate of $p_c(L)$.

Figure 11(a) shows the results of plotting $[p_c(L)-p_c(\infty)]$ as a function of $\log(L)$. The slope of the resulting line leads to an estimate of $\nu=0.93\pm0.03$, which is within 6% of the canonical value listed in Table I.

The ratio of β/ν is determined by examining the finite-size scaling of the size of largest cluster at the critical point [23] via

$$s_{\max}/L^d\sim L^{\beta/\nu}, \tag{11}$$

where $s_{\max}$ is the size of the largest cluster and d is the Euclidean dimension of the lattice. Figure 11(b) shows this plot for percolation lattices with $L=3$, 4, 5, 6, 22, and 63. This method leads to $\beta/\nu=0.44\pm0.01$, which is within 7% of the canonical three-dimensional lattice value of $\beta/\nu=0.47$.

VIII. CONCLUSION

The scaling function for three-dimensional percolation has been determined from data for a lattice of side $L=6$. Using the scaling function, the γ-power law for three-dimensional percolation was derived. Theoretically, this power law should describe the divergence of the second moment in the critical region for any percolation lattice in three dimensions, regardless of lattice geometry and independent of system size, at least to a lower limit of $L=3$. This is born out by the agreement between the predicted power law, derived from the scaling function of three-dimensional percolation obtained for the $L=6$ lattice, and the behavior of the second moment from the $L=63$ lattice. Thus, behavior of a large lattice has been predicted based on the analysis of a small lattice. The power law predicted using the scaling function also describes the second moment data from the $L=6$ lattice over some critical range. This critical range is the same range that was used in the prior analysis of $L=6$

lattices [14]. Using the γ-matching methods employed during the extraction of critical exponents from multifragmentation data [11] the same critical regions were found. The agreement of the size and location of the critical regions and the agreement of the values of the extracted exponent with the infinite lattice value indicates that the γ-matching method is sound and can be used to determine the values of bulk matter critical exponents from small systems.

It was also shown that it is possible to observe critical behavior in the $L=6$ lattice when the cluster multiplicity was used as the control parameter rather than the lattice probability. The relationship between M and p_l is not linear, but did not significantly affect the scaling behavior of the cluster distribution. A scaling function was determined and the γ-power law was determined. This power law predicted the second moment behavior for the $L=63$ lattice as well as for the $L=6$.

Finally, the effects of the finite system size were examined for lattices with sizes that varied more than four orders of magnitude. The power laws predicted by finite-size scaling theory were observed. The values of critical exponents determined from these power laws agreed well with infinite lattice values.

Table I summarizes the results from the work of [14] for the $L=63$ lattice, the $L=6$ lattice, and the results from this study for finite-size scaling and compares them with the infinite lattice results for three-dimensional percolation. The agreement of the quantities determined by examining small lattices is generally within 10% of the accepted values. This indicates that critical behavior is indeed present in systems with as few as 27 constituents using the intrinsic control parameter (p_l for percolation) or another measure of the distance from the critical point such as cluster, or charged particle multiplicity. These techniques of cluster analysis can now be applied to the fragment distributions of nuclear multifragmentation.

This work was supported by the U.S. Department of Energy under Contract No. DE-FG02-88ER40408.

[1] A. M. Poskanzer *et al.*, Phys. Rev. C **3**, 882 (1971).
[2] G. D. Westfall *et al.*, Phys. Rev. C **17**, 1368 (1978).
[3] J. A. Gaidos *et al.*, Phys. Rev. Lett. **42**, 82 (1979).
[4] J. E. Finn *et al.*, Phys. Rev. Lett. **49**, 1321 (1982).
[5] R. W. Minich *et al.*, Phys. Lett. **118B**, 458 (1982).
[6] X. Campi, J. Phys. A **19**, L917 (1986).
[7] X. Campi, Phys. Lett. B **208**, 35l (1988).
[8] W. Bauer, Phys. Rev. C **38**, 1297 (1988).
[9] J. Hebele *et al.*, Z. Phys. A **340**, 263 (1991).
[10] P. Kreutz *et al.*, Nucl. Phys. **A556**, 672 (1993).
[11] M. L. Gilkes *et al.*, Phys. Rev. Lett. **73**, 1590 (1994).
[12] J. B. Elliott *et al.*, Phys. Lett. B **381**, 35 (1996).
[13] J. A. Hauger *et al.* Phys. Rev. Lett. **77**, 235 (1996).
[14] J. B. Elliott *et al.*, Phys. Rev. C **49**, 3185 (1994).
[15] D. Stauffer, Phys. Rep. **54**, 2 (1979).
[16] H. Nakanishi and H. E. Stanley, Phys. Rev. B **22**, 2466 (1980).
[17] X. Campi, *Fragmentation of Clusters, Proceedings of the International School of Physics* (Italian Physical Society, Varenna, 1990).
[18] A. D. Panagiotou *et al.*, Phys. Rev. Lett. **52**, 496 (1984).
[19] W. Bauer *et al.*, Phys. Lett. **150B**, 53 (1985).
[20] T. Li *et al.*, Phys. Rev. Lett. **70**, 1924 (1993).
[21] T. Li *et al.*, Phys. Rev. C **49**, 1630 (1994).
[22] S. Das Gupta and J. Pan, Phys. Rev. C **53**, 1319 (1996).
[23] D. Stauffer and A. Aharnony, *Introduction to Percolation Theory*, 2nd ed. (Taylor and Francis, London, 1985).
[24] D. W. Heermann and D. Stauffer, Z. Phys. B **44**, 339 (1981).